Article:

Mawodza, T., Menon, M. orcid.org/0000-0001-5665-7464, Brooks, H. et al. (3 more authors) (2021) Preferential wheat (Triticum aestivum. L cv. Fielder) root growth in different sized aggregates. Soil and Tillage Research, 212. 105054. ISSN 0167-1987

https://doi.org/10.1016/j.still.2021.105054

Preferential wheat (Triticum aestivum. L cv. Fielder) root growth in different sized aggregates

Tinashe Mawodza*[a], Manoj Menon[a], Harriet Brooks[a], Oxana V. Magdysyuk[b], Genoveva Burca[c], Stuart Casson[d],

[a] Department of Geography, The University of Sheffield, Sheffield S10 2TN, United Kingdom

[b] Diamond Light Source Ltd, Harwell Science and Innovation Campus, Didcot, OX11 0DE, United Kingdom

[c] STFC, Rutherford Appleton Laboratory, ISIS Facility, Harwell, OX11 0QX, United Kingdom

[d] Department of Molecular Biology and Biotechnology, The University of Sheffield, Sheffield S10 2TN, United Kingdom

*Corresponding author email: t.mawodza@sheffield.ac.uk

Abstract

Soil structure is one of the most important environmental factors affecting root architectural development and consequently plant yield. Understanding how plant roots respond to soils with variable soil structure is important as it enables soil management practices that promote optimal root growth. Many contemporary, non-invasive experiments investigating how plant root architecture responds to soil structural variations have often focused on compaction, often neglecting the role of soil aggregate size in determining root configuration. To better understand this, in this study, we used non-invasive neutron and X-Ray imaging to investigate how variable aggregate size affects the early root architectural establishment in wheat plants. Sandy loam soil derived macro-aggregates of two distinct sizes (0.25-0.5 and 2-4 mm) were used to infer the suitability of each aggregate size for use in wheat seedbeds. We also grew wheat seedlings in partitioned containers with the two different aggregate size classes filled side by side to establish whether there would be preferential growth of roots in either aggregate size class. Our results showed significantly increased root growth in the smaller 0.25-0.5 mm aggregates as compared to the larger 2-4 mm aggregates. This was mainly as a result of enhanced lateral root growth when the wheat plants were grown in the finer aggregates. On the other hand, coarser aggregates induced significantly increased seminal root axes which partially offset the differences in total root length between the two aggregate sizes. Plants growing in partitioned containers similarly indicated preferential root growth in smaller aggregate with an even more pronounced difference in root growth in the smaller aggregates. As inferred from our results, seedbeds dominated by smaller macro-aggregates (finer soil tilth) may be optimal to enhance wheat seedling root growth in sandy loam soils.

Keywords: Soil aggregates, Soil Structure, Neutron computed tomography, X-Ray computed tomography

1. Introduction

Even though they are often obscured underground, roots are an integral component of a plant's complex physiology. They are responsible for numerous functions such as anchorage, aeration, carbohydrate storage and most importantly, the acquisition of essential resources, namely water and nutrients from growth substrates (most commonly soil). Since both water and plant nutrients are usually unevenly distributed within soil, roots often have to forage to acquire these resources (Lynch 2019). As a result of this foraging, root systems inherently show a great deal of plasticity which is governed by both environmental and genetic cues that optimise them for resource acquisition (Topp 2016, Suralta *et al.* 2018, Fromm 2019). Understanding how these factors affect root growth and architecture is essential for the improvement of agricultural productivity as plant yield and vigour is often directly related to root performance (Wang *et al.* 2020).

Of all the environmental factors affecting root growth, soil structure is one of the most salient as it directly influences the movement and distribution of water, air and heat as well as roots themselves (Bronick and Lal 2005). Soils with a poor structure often exhibit severely limited productivity as a result of suboptimal pore size distribution and connectivity (Nimmo 2004). As soil aggregates have a direct bearing on a soil's pore characteristics, their stability and distribution are often used as a proxy for soil structural integrity. To improve aggregation and thereby soil structure in the long term, strategies such as reduced tillage, crop rotation, cover crops as well as the addition of organic matter and conditioners are often carried out. Tillage itself, despite the criticism associated with its prolonged use, is also often used to improve the temporal structure of soils for good early root establishment (Bronick and Lal 2005, Jabro *et al.* 2015, Bahmani 2019). This is because it breaks down large clumps of soil (clods) into smaller aggregates and individual particles which ensure good seed-soil contact in the seedbed as well as an ideal pore network for root growth (Snyder and Vázquez 2005, Blunk *et al.* 2017).

Identifying the optimal tilth required for plant growth is important as more than 70% of roots of most crops grow within the often cultivated top 15-30cm of soil (Braunack and Dexter 1988). Experimentally, however, determining optimal soil tilth is challenging due to the difficulty of replication of post tillage field soil conditions accurately (Braunack 1995). In account of this, soil aggregates of different size classes are often used as a standardised proxy to characterise the ideal soil tilth required for plant growth (Braunack and Dexter 1989). These distinct aggregate size classes often present unique structural differences between the soils under review thus allowing for the response of roots to different structures to be characterised. For instance, larger soil aggregates generally present a structure with larger inter-aggregate pores that allow for increased movement of water, heat and air whilst reducing root-soil contact. On the other hand, finer soil aggregates have much smaller inter-aggregate pores that limit the bulk mobility of elements different via mas water flow but allow for better root-soil contact that often increases plant nutrient availability (Snyder and Vázquez 2005).

In terms of the mechanics of root growth into these different sized aggregates, three possible fates are most likely (Dexter and Hewitt 1978, Hewitt and Dexter 1984, Whiteley and Dexter 1984). The first possibility is that the root is able to push the aggregate or soil particle out of its path, maintaining its trajectory. This is usually the case when roots grow in soil of low strength such as soil composed of small loosely connected aggregates or moist soil (Clark and Barraclough 1999, Ball *et al.* 2005, Bodner *et al.* 2014). The second possible fate would be to penetrate the aggregate, which normally occurs when the aggregate is larger than the root diameter and cannot displace it out of its path due to strong bonding between the aggregate and the other surrounding aggregates. In this case, the growing root preferentially forces itself through a plane of weakness in the encountered aggregate (Stirzaker *et al.* 1996, Ball *et al.* 2005). The third possibility occurs when the root cannot displace the encountered aggregate out of its path whilst the aggregate is of relatively higher strength and has little or no plane of weakness. In this event the root first attempts to force itself through the aggregate by exerting axial strength. When the root reaches its maximal axial strength, it then buckles (often increasing root thickness) and is subsequently deflected around the soil aggregate (Whiteley *et al.* 1982, Logsdon *et al.* 1987, Logsdon 2013). This also occurs when roots encounter an aggregate at an angle greater than 90°. In practice, however, these mechanisms of root growth into the soil are not mutually exclusive and an intermediate behaviour usually occurs (Whiteley and Dexter 1984).

To understand how these mechanisms work in determining root growth in aggregates of different sizes, experimentation is vital. Accordingly, several different studies have been carried out to understand root growth in different structures with aggregates of sizes ranging between 250 μm up to 20 mm being used in both pot and field experiments investigating plants from different species (Hadas 1975, Braunack and Dexter 1988, Alexander and Miller 1991, Braunack 1995, Nakamoto 2002). For wheat specifically, there is considerable variability in the studies reporting optimal aggregate size for germination and root growth. Aggregates ranging between 1 and 2 mm were reported to produce superior germination as compared to other aggregate size classes (Dojarenko 1924, Jaggi et al. 1972, Braunack and Dexter 1989). On the other hand, Kvasnikov (1928) found that 2-3 mm aggregates performed better than the 1-2 mm aggregates. On the extreme ends, Håkansson and von Polgár (1984) also showed that wheat roots performed best in the aggregates size class <1 mm especially under water-limited conditions whilst Hagin (1952) showed that aggregates >2 mm were more optimal for wheat root growth. All these studies, however, although informative used destructive and invasive root washing which limits conclusions that can be made in terms of specific root architectural development as compared to non-invasive imaging techniques (Tracy *et al.* 2010, Mairhofer *et al.* 2017). On the contrary, in a recent experiment, Mawodza et al. (2020) used non-invasive neutron imaging and visualised a distinct pattern of wheat root distributions in randomly segregated different aggregates indicating a reduction in lateral root growth in larger aggregates.

Another important consideration when investigating root growth in different sized aggregates is the role that different type of roots play in resource acquisition and distribution. In the early growth of wheat plants, seminal roots which are roots that emanate from the seed embryo are the thickest and most distinct root types. These are partnered by smaller lateral roots of different orders which emanate from the seminal roots themselves and often grow perpendicular to their parent seminals. The potential for resource extraction among these different type of roots is dependent on their thickness and distribution with thicker roots more responsible for bulk water flow whilst finer roots contribute more to resource acquisition from soil (Zarebanadkouki *et al.* 2013). As such the thicker seminal roots are mainly responsible for bulk transport whilst finer lateral roots branching from these seminal are thought to be responsible for the bulk of the water and nutrient acquisition. The distribution and abundance of these roots in soils of different sized aggregates would give an indication of the extent and location of resource acquisition in each media.

In this study, we investigate wheat root growth in aggregates of different size classes using non-invasive neutron and X-ray imaging. Based on the studies described above, we hypothesize that root growth would be better in smaller aggregates as compared to the larger aggregates. We also look at how wheat plants respond to growth in a partitioned experiment with the plant having the possibility of growth in either of two different aggregate size classes. This novel approach would give us an idea of the potential preferential root growth in aggregates of different size classes using non-invasive neutron computed tomography (NCT).

2. Materials and methods

2.1 Soil properties

The soil used in this study was a sandy loam soil (70% Sand, 16% Clay, and 14% Silt) obtained from Cove Farm (53°30'03.7"N 0°53'57.2"W) with an organic carbon content of 4.18 ± 0.18 %. This soil was air-dried and mechanically sieved through a nest of sieves to obtain several macro aggregate fractions which were subsequently used for experimentation (including preliminary experiments). Selected chemical properties of the sieved bulk soil (sieved to 4mm), as well as the various sieved aggregate fractions, are described in Table 1.

2.2 Assessment of root growth differences in selected aggregates

2.2.1 Root growth in individual aggregate size classes

In the first experiment, two of the selected aggregate fractions (2-4 mm and 0.25-0.5 mm) were packed into bottom sealed cylindrical 1mm walled aluminium tubes (18 mm inner diameter × 100 mm height) to attain bulk densities of 1.2 g cm^{-3} for the 0.25-0.5 mm size aggregates and 0.92 g cm^{-3} for the 2-4 mm aggregates. A single wheat seed was then sown 10 mm underneath the surface of the aggregates and irrigation was applied to a gravimetrically determined volumetric moisture content (θ_v) of 16% with at least 5 replicates for each aggregate treatment. The wheat in the aggregate filled tubes was then grown in a growth chamber maintained at 21°C (day)/18°C (night) and 50% relative humidity. The above-mentioned moisture content was maintained by watering the tubes every day until 5 days before neutron imaging when they were allowed to dry to increase root/soil contrast during imaging. Plants were grown for 14 days before neutron imaging was carried out.

2.2.2 Partitioned aggregate experiment

The second experiment comprised of the same two aggregate sizes used in the first experiment, however, these were alternatively poured into different sides of square prisms (20 mm ×20 mm; h= 100 mm) separated by cardboard. The prism shape is preferred over a cylinder so that the cardboard can be placed diagonally and securely while filling aggregates. This set up is illustrated in Figure 1. After careful filling of the container to within 5 mm of the brim, the cardboard partition was gently removed by pulling it slowly upwards, preserving the separation of the differently sized aggregates. A single wheat seed was planted at the centre of each of the containers such that the seed was in contact with both aggregates at planting. Watering was done every day with a syringe being used to individually irrigate each aggregate partition. This watering at first was done to ensure that each of the partitions received the equivalent of a gravimetrically determined θ_v of 16% as in the first experiment. This was subsequently daily maintained by adding half of the gravimetrically estimated amount of water lost to each partition. Similar to the first plant experiment, plants were also grown for 14 days with watering being stopped 5 days prior to neutron imaging.

2.3 Root and soil imaging

2.3.1 Neutron computed tomography (CT) for root analysis

Neutron imaging was carried out at the IMAT neutron imaging and diffraction facility of the ISIS neutron spallation source at the Rutherford Appleton Laboratory (UK) (Burca *et al.* 2018) using an optical camera box equipped with a 2048 × 2048 pixels Andor Zyla 4.2 PLUS sCMOS camera for a standard white beam neutron tomography with 0.7-7 Å energy range.. Scanning was performed following a modified version of the protocol similar to that described in Mawodza *et al.* (2020) and Mawodza (2019). Six of the strongest plants were measured in the first neutron imaging experiment and two plants in the second (partitioned) experiment.. For the first experiment, the scanning of the cylindrical containers was done with a rotation step of 0.55° for each projection with an exposure time of 30sec per radiography resulting in 654 projections over 6 hours of measurement with an effective pixel size of 55µm. for a field-of-view of 112.7 mm × 112.7 mm. For the second experiment, however, due to the shape of the square-shaped prisms that had a thicker cross-section, an increased number of projections were collected which increased the image acquisition time of 10 hours with 966 projections being taken with a rotation step of 0.373° for each projection. A multiaxial tomography stage available on the IMAT, which allowed for two simultaneously scans, was employed during this experiment for an efficient use of the beamtime allocated.

2.3.2 Neutron image processing

The neutron radiographies acquired were first cropped in NIMH Image J v1.50g (Schneider *et al.* 2012) to crop out the alternate plant images from the same scan. These cropped images were then imported into Octopus 8.9 reconstruction software (Octopus 2019) which was then used to correct for neutron beam variation and camera noise using the flat images and dark images taken before and after image acquisition. This is done using the formula:

$$I' = N.\frac{I_{raw} - I_{dark}}{I_{open\ beam} - I_{dark}}$$

Where I_{raw} is the raw image, I_{dark} is the image devoid of sample and beam, $I_{open\ beam}$ is the open beam image containing beam characteristics without sample.

The corrected images were then reconstructed into a stack of .tiff files which were then imported into Avizo ® 9.0.1 (FEI 2015) for segmentation and analysis. To get the best results of segmentation, roots were manually segmented using a limited range paintbrush editor in the segmentation module in the software. Segmentation took an average of 4 hours per plant to complete. The segmented roots obtained from this process were then used to calculate root lengths, thickness, surface area and volume for each root scan. Seminal root tortuosity was estimated using the formula

$$\tau = \frac{L}{D}$$

Where L is the seminal root length and D is the straight line distance between the seed-root intersection and the root tip (Schwarz *et al.* 2010). Relative moisture distribution from NCT in plant samples was done to estimate the amount of water retained by each aggregate size at the time of imaging. This was calibrated for by using identical cylinders containing the same soil type at different moisture contents to ensure that the relative moisture content could be quantified.

2.3.3 Flatbed scanning and WinRhizo® root analysis and biomass determination

Subsequent to neutron scanning, all the plants that were grown (including extra replicates) were destructively removed from their tubes and the soil attached to the roots was washed off over running water with a 2 mm size mesh. The cleaned roots were then placed into a transparent water-filled tray and scanned at 600 dpi using an Epson Expression 10000XL Pro flatbed scanner. The images produced were then analysed using WinRhizo® 2016a software (Arsenault *et al.* 1995, Wang and Zhang 2009). This analysis produced information on root length, thickness, volume and surface area. After this analysis, the roots were then excised from the shoot then both were dried at 60°C for 24 hours in an oven and weighed to determine dry root and shoot biomass.

2.3.4 X-Ray synchrotron imaging of soil aggregates

As aggregate size and packing influences pore size distribution and ultimately root growth patterns, it was vital to investigate the pore size distribution produced by each macro aggregate size class used in our experiment. Since the neutron imaging is not sensitive to most of the soil components responsible for soil structural differentiation (such as silica and aluminium), the use of non-invasive X-Ray imaging was key to obtaining detailed understanding of the pore and particle distribution within the plant growth tubes used in this study. As such, similarly packed plastic tubes containing aggregates of the two aggregate size classes (0.25-0.5 and 2-4 mm) were scanned using high-resolution X-ray synchrotron imaging. This was done at the I12-JEEP beamline (Drakopoulos *et al.* (2015) at the Diamond Light Source facility (UK). The soil columns were scanned using a monochromatic beam with an image resolution of 1.3 µm per pixel. The scans covered a volume of 19.77 mm^3 within in each column. Tomographic reconstruction was performed using the SAVU system (Atwood *et al.* 2015, Wadeson and Basham 2016). A filtered back projection (FBP) algorithm was used (Ramachandran and Lakshminarayanan 1971), as implemented in the ASTRA toolbox (van Aarle *et al.* 2016). A combination of greyscale based image thresholding augmented by manual segmentation as described in Menon *et al.* (2020) was used to delineate between soil particles and air spaces. The segmented images were then used to estimate the inter- and intra-aggregate pores within each of the scanned soil columns. For this study, although the complementary use of both X-Ray and neutron CT for each of the specimens would have been more ideal to reveal a more detailed association between root and soil structural features, this was however, not done as the imaging using the two techniques could not be carried out concurrently due to logistical constraights.

2.3.5 Statistical analysis

The statistical analyses for these experiments were performed using GraphPad Prism 8.0.1 (San Diego, California USA, www.graphpad.com). Two-tailed T-tests were used to separate between means.

3. Results

3.1 Plant biomass production

The total biomass produced by wheat seedlings grown in the smaller aggregate size class (0.25-0.5 mm) was significantly greater as compared to those grown in the larger aggregates (2-4 mm) with on average, an increase of 25% in the smaller aggregate size. In the larger aggregates, only root biomass was significantly reduced with 31% lower root dry mass as compared to the smaller sized aggregates as is illustrated in Figure 2a. Shoot biomass in the larger aggregates was also reduced by about 19%, although this difference was not statistically significant. In terms of shoot: root ratio, there was a significant difference between plants growing in the two aggregate size classes with the smaller aggregates showing a comparatively higher (0.833 ± 0.041) ratio as compared to those growing in the larger aggregates (0.692 ± 0.104).

3.2 Root architectural properties in different aggregates

Root metrics and 3D volume-rendering were obtained from NCT while WinRhizo® measurements being used to validate data from the non-invasive imaging. The total root system length grown in the two different aggregates was comparable with no significant difference in plants grown in either size class as illustrated in Figure 3a. Root growth patterns were however distinct, with plants growing in the smaller aggregates exhibiting significantly increased lateral root growth as compared to the larger aggregates. Plants growing in the larger aggregates on the other hand, had more abundant seminal roots, which somewhat compensated for the reduced lateral roots, this is illustrated in Figure 3a and Figure 4. There were also no significant differences in root thickness between plants grown in the different aggregates, however, plants grown in larger aggregates had marginally thicker (448 ± 47 µm) roots as compared to plants grown in the smaller aggregates (411 ± 32 µm). Root tortuosity was also significantly lower in the smaller aggregate size class as illustrated in Figure 3b.

3.3 Root growth in partitioned aggregates

The results from the partitioned tube experiment showed a similar trend to those shown in the experiment where wheat seedlings were grown in the aggregate size classes separately. As detailed in Table 2, root length in the larger aggregate size class was 38- 49% shorter than those in the smaller aggregate size class. Other root properties such as root surface area and volume also followed a similar trend being almost double in the smaller aggregates as compared to the larger aggregates. Lateral root growth in the smaller aggregates also showed preferential growth in the smaller aggregates with differences being clearly visible in the 3D renderings in Figure 5. The wheat seedlings also all had 5 seminal roots similar to what was observed in the previous experiment when plants were grown in the larger aggregates, even though aggregate of both size classes were used.

3.4 Water distribution in the different aggregate size classes

During neutron imaging, the water content of the growth tubes containing the different aggregates varied significantly with the larger aggregates retaining much greater amounts of water compared to the smaller aggregates, as shown in Figure 6a. Soil moisture content also increased towards the base of each of the growth tubes for both aggregate size classes with roots near the base of the container being most pronounced especially in the smaller aggregates, mainly as a result of increased moisture lower down the soil column. Roots growing in the larger aggregate sizes also showed variable moisture content depending on their interaction with the moist aggregates. As such roots traversing through the large inter aggregate pores in the large aggregates showed relatively lower moisture contents within the pores indicating a reduction in moisture levels when they passed through them as demonstrated in Figure 6b.

3.5 Pore distribution

The pore size distribution in the two aggregate size classes was distinctly different with the 0.25-0.5 mm aggregates having relatively fewer intra-aggregate pores as compared to the larger 2-4 mm aggregates. The 0.25-0.5 mm aggregate size class was made up of numerous coarse sized sand particles in addition to similarly sized aggregates that tended to reduce the smaller intra-aggregate pores in this fraction. The inter-aggregate pores in the 2-4 mm aggregate size fraction were also much larger and more continuous, making up the largest proportion of pores in this fraction. An illustration of the pore distribution in the different aggregate size classes is given in Figure 7 with metrics from these volumes being given in Table 3.

4. Discussion

The use of non-invasive neutron imaging, namely NCT, in this study represents a novel approach of looking at root growth in different aggregate size classes as previously, studies looking into root architectural differences only used destructive methods of studying root-aggregate interactions. These, although being useful, are not able to capture the three-dimensional architectural differences to reveal how roots interact with aggregates and often underestimate roots due to losses at washing. Our results revealed that wheat seedlings growing in the finer aggregates showed marginally increased root length as compared to the coarser aggregates despite distinct differences in root biomass. A more detailed analysis of the root growth patterns revealed that this marginal difference was attributed to enhanced numbers of lateral root primordia in the finer aggregates as compared to the coarser aggregates. This may have arisen as a consequence of better root-soil contact in the finer aggregates which had the effect of improving lateral root initiation leading to increased hydropatterning (Orosa-Puente *et al.* 2018). In the coarser aggregates, on the other hand, lateral root initiation was visibly limited with fewer but longer lateral roots growing. The large inter aggregate pores as observed in the X-Ray tomography images of coarse aggregates may have discouraged lateral root initiation as they would have to transverse large swathes of air to reach moist soil which is undesirable for root resource acquisition (Stirzaker *et al.* 1996). The large pores similarly also mimic bio pores which have been shown to encourage axial root expansion at the expense of lateral root growth (Ball *et al.* 2005). Our results are similar to what was observed by Logsdon *et al.* (1987), Alexander and Miller (1991) as well as Donald *et al.* (1987) who also reported a preference for axial root elongation as opposed to lateral root system expansion in larger aggregates for maize. This axial elongation has also been shown to increase the ability of roots to penetrate much deeper layers of soil to access moisture (Clark and Barraclough 1999, White and Kirkegaard 2010, Gao *et al.* 2016). As a consequence, coarse aggregates may be ideal in environments where surface dryness often persists and plants have to forage for water deeper in the soil profile.

In terms of biomass, productivity in smaller aggregates was enhanced as compared to that in the larger aggregates. This was as exemplified by the differences in root and shoot biomass production of wheat seedlings growing in each aggregate size class. The observed differences could be explained by in several ways, firstly looking at the soil chemical analysis, there was 68% difference in the phosphorus concentration between the two aggregates which may have resulted in improved root biomass production in the smaller aggregates as P deficiencies are known to enhance root foraging for the element. Secondly the differences in bulk density between the two different aggregate sizes (0.92 vs 1.2) resulted in more soil material being available for resource acquisition thus potentially improving root growth in the smaller aggregate size with higher bulk density. Furthermore improved root-soil contact may have also played a role in improving plant growth. Our results are similar to the results obtained by Misra *et al.* (1986a), Donald *et al.* (1987), Logsdon *et al.* (1987) and Alexander and Miller (1991) who also reported improved shoot and root growth in finer aggregates. These results are however, contrary to the findings by Agrawal *et al.* (1984) as well as Agrawal and Jhorar (1987) who showed better root growth in wheat plants growing in large aggregates (>2mm) over a 12 week period. The improved root growth in smaller aggregates in our experiment was thought to be a result of a variety of factors such as improved root-soil contact, improved nutrition as well as general ease of root penetration as roots required smaller amounts of energy to deflect smaller aggregates as opposed to the larger aggregates (Dexter 1978).

The high root to shoot ratio in the smaller aggregates in our experiments suggested that the seedlings growing in this media could have experienced increased moisture deficiency as periodic droughting is known to increase root: shoot ratio (Xu et al. 2015). Further evidence of this may lie in quicker drying in the smaller aggregates as indicated by the lower soil water content observed during NCT imaging which could lead to temporal moisture deficiencies. The drying, however, may also be explained by increased plant growth contributing to improved water uptake which in turn contributes to increase foraging. It is worth noting however, that moisture variations as estimated by neutron imaging do not represent absolute moisture contents and may overestimate moisture contents due to hydrogen rich materials within the soil such as organic matter within soils (e.g. from mucilage or soil organic matter). Differences in root: shoot ratio may also have been due to plants growing in smaller aggregates experiencing a higher degree of phosphorus deficiency as increased root growth in preference to shoots is often attributed to plants foraging for the element (Lynch 2007, Bhattacharya 2019). It noteworthy however, that wheat germination and initial early root growth is predominantly externally influenced by soil physical properties which govern factors such as access to aeration, moisture and soil temperature (Bouaziz and Hicks 1990, Bouaziz et al. 1990, Poole 2016). Soil nutrition although important only begins to play a dominant role after the initial stages growth when seed resources begin to deplete which is why seed size and weight controls early growth and vigour in wheat and other species (Ries and Everson 1973, Puri and Qualset 1978, Abd El Rahman and Bourdu 1986).

Interactions between plant roots and different soil structures as derived from growth in different soil aggregates also revealed seminal root tortuosity of the plants grown in the smaller aggregates were smaller, indicating shorter paths of downward trajectory as the seminal roots entered into the soil. This could be explained by the fact that in the smaller aggregates, roots could more easily deflect them and continue their downward trajectory (Misra *et al.* 1986b, 1988, Popova *et al.* 2016). There was, however, no difference in root thickness in plants growing in both aggregates suggesting that roots in the larger aggregates did not often buckle when attempting to enter the large aggregates as has been demonstrated in other experiments such as the increased radial root expansion shown by Logsdon *et al.* (1987) and Logsdon (2013) in maize plants. This may be due to the increased porosity in our experiment, which allowed the roots to grow freely around the large aggregates instead of penetrating them.

The partitioned root experiment provided a novel approach of looking at root growth in aggregates with no previous experiments in literature having elaborately been able to show root behaviour at the transition between different aggregate size classes. Root growth patterns were largely coherent to those shown when the seedlings were grown in single aggregates. This indicated that similar processes governed root growth in this setup. As such, preferential root growth was prevalent with the finer aggregates having almost double the root length as compared to the coarser aggregates. The abrupt soil structural change brought about by the transition between different aggregate size classes did not seem to affect root growth paths with roots not visibly changing direction at the transition between these zones. Seminal root growth in the partitioned growth tubes was similar to what happened in the larger aggregates with both plants having five seminal roots as opposed to an average of three in the finer aggregates. This could have been due to the influence of the coarser aggregates that tend to encourage axial growth in preference to lateral root growth (Clark and Barraclough 1999, White and Kirkegaard 2010). This is primarily due to the notable absence of non-invasive imaging when studying plants growing in different aggregate sizes. Non-invasive imaging was paramount in this experiment as separating roots for analysing architectural differences destructively would be difficult without disturbing the root distribution patterns. Other related experiments investigating how plant roots interact with soil structure that uses non-invasive imagery mainly focus on root growth in relation to compaction. For instance, Tracy *et al.* (2012), Popova *et al.* (2016) and Burr-Hersey *et al.* (2017) all showed non-invasively how roots behaved when growing in soils with compaction but did not, however, show root behaviour specifically in relation to different aggregates.

In terms of segmentation, NCT images in the larger aggregates were much easier to segment as compared to those in the smaller aggregates even though they were much drier at the time of imaging. This was primarily because the smaller lateral roots seemed to dry along with the soil thus reducing their contrast with the soil. This is similar to what was reported by Mawodza *et al.* (2020) who showed variable water distribution throughout the roots with reduced moisture especially in roots growing through pores. As soil structure was key in this particular experiment, the use of NCT in conjunction with X-Ray CT experiment would have been more informative. This would have enable us to study both plant roots and soil structure simultaneously due to their complementarity (Robinson *et al.* 2008, Moradi *et al.* 2013, Karch *et al.* 2017). This was, however, not possible as facility access was limited and we couldwith only use NCT to study plant soil-interactions. NCT also has its own limitations such as the relatively low resolution that can make it difficult to segment the smaller lateral roots. As such to counteract this, we used flatbed scanning to provide additional information on the smaller features that may have been missed using NCT.

5. Conclusions

In this study, we present a novel approach of investigating the interactions between soil aggregates and roots in three dimensions using NCT. Our results clearly showed improved root growth in smaller macro-aggregates as opposed to larger aggregates. These findings may have implications in terms of soil cultivation with soils containing finer macroaggregates (finer tilth) being recommended for the better establishment of wheat plants growing in well watered sandy loam soils. For deeper root growth especially in water limited conditions however, soils with larger aggregates may be more ideal as this promotes better axial growth allowing roots to penetrate deeper into the soil for better water acquisition. As soils in nature are unlikely to segregate into distinct sizes as it was the case with the one used in this study, to further enhance our undertanding of root-aggregate interactions in soils in their natural state, future research into cultivated soils with a more extensive range of aggregates may be required to further determine how wheat plants respond to a wider variety of aggregates in agricultural soils.

Acknowledgements

This research was funded as part of a PhD studentship by the Grantham Centre for Sustainable Futures at the University of Sheffield. Neutron imaging beamline grant (RB1820361) was provided by STFC ISIS Facility (doi: 10.5286/ISIS.E.RB1820361) as well as the I12 beamline (proposal mg22992) at Diamond Light Source Ltd., UK.

References

van Aarle, W., Palenstijn, W.J., Cant, J., Janssens, E., Bleichrodt, F., Dabravolski, A., De Beenhouwer, J., Joost Batenburg, K., and Sijbers, J., 2016. Fast and flexible X-ray tomography using the ASTRA toolbox. *Optics Express*, 24 (22), 25129.

Abd El Rahman, N. and Bourdu, R., 1986. Effet de la taille et de la forme des grains sur quelques caractéristiques du développement du maïs au stade jeune. *Agronomie*, 6 (2), 181–186.

Agrawal, R.P. and Jhorar, B., 1987. Soil Aggregates and Growth of Wheat. *J. Agronomy & Crop Science*, 158, 160–163.

Agrawal, R.P., Mundra, M., and Jhorar, B.S., 1984. Seedbed tilth and nitrogen response of wheat. *Soil & Tillage Research*, 4, 25–34.

Alexander, K.G. and Miller, M.H., 1991. The effect of soil aggregate size on early growth and shoot-root ratio of maize (Zea mays L.). *Plant and Soil*, 138 (2), 189–194.

Arsenault, J.-L., Poulcur, S., Messier, C., and Guay, R., 1995. WinRHIZO™, a Root-measuring System with a Unique Overlap Correction Method. *HortScience*, 30 (4), 906D – 906.

Atwood, R.C., Bodey, A.J., Price, S.W.T., Basham, M., and Drakopoulos, M., 2015. A high-throughput system for high-quality tomographic reconstruction of large datasets at diamond light source. *Philosophical Transactions of the Royal Society A: Mathematical, Physical and Engineering Sciences*, 373 (2043).

Bahmani, O., 2019. Evaluation of the short-term effect of tillage practices on soil hydro-physical properties. *Polish Journal of Soil Science*, 52 (1), 43–57.

Ball, B.C., Bingham, I., Rees, R.M., Watson, C.A., and Litterick, A., 2005. The role of crop rotations in determining soil structure and crop growth conditions. *Canadian Journal of Soil Science*, 85 (5), 557–577.

Bhattacharya, A., 2019. Changing environmental condition and phosphorus-use efficiency in plants. *Changing Climate and Resource Use Efficiency in Plants; Academic Press: Cambridge, MA, USA*, 241–305.

Blunk, S., Malik, A.H., de Heer, M.I., Ekblad, T., Bussell, J., Sparkes, D., Fredlund, K., Sturrock, C.J., and Mooney, S.J., 2017. Quantification of seed-soil contact of sugar beet (Beta vulgaris) using X-ray Computed Tomography. *Plant Methods*, 13 (1), 1–14.

Bodner, G., Leitner, D., and Kaul, H.P., 2014. Coarse and fine root plants affect pore size distributions differently. *Plant and Soil*, 380 (1), 133–151.

Bouaziz, A. and Hicks, D.R., 1990. Consumption of wheat seed reserves during germination and early growth as affected by soil water potential. *Plant and Soil*, 128 (2), 161–165.

Bouaziz, A., Souty, N., and Hicks, D., 1990. Emergence force exerted by wheat seedlings. *Soil and Tillage Research*, 17 (3–4), 211–219.

Braunack, M.., 1995. Effect of aggregate size and soil water content on emergence of soybean (Glycine max, L. Merr.) and maize (Zea mays, L.), 33, 149–161.

Braunack, M.. and Dexter, A.., 1988. The Effect of Aggregate Size in the Seedbed on Surface Crusting and Growth and Yield of Wheat (Triticum aestivum L., cv. Halberd) Under Dryland Conditions, 11, 133–145.

Braunack, M.. and Dexter, A.., 1989. Soil Aggregation in the Seedbed: a Review. II. Effect of Aggregate Sizes on Plant Growth M.V. *Soil & Tillage Research,* 14, 281–298.

Bronick, C.J. and Lal, R., 2005. Soil structure and management: A review. *Geoderma*, 124 (1–2), 3–22.

Burca, G., Nagella, S., Clark, T., Tasev, D., Rahman, I.A., Garwood, R.J., Spencer, A.R.T., Turner, M.J., and Kelleher, J.F., 2018. Exploring the potential of neutron imaging for life sciences on IMAT. *Journal of Microscopy*, 00 (0), 1–6.

Burr-Hersey, J.E., Mooney, S.J., Bengough, A.G., Mairhofer, S., and Ritz, K., 2017. Developmental morphology of cover crop species exhibit contrasting behaviour to changes in soil bulk density, revealed by X-ray computed tomography. *PLoS ONE*, 12 (7), 1–18.

Clark, L.J. and Barraclough, P.B., 1999. Do dicotyledons generate greater maximum axial root growth pressures than monocotyledons? *Journal of Experimental Botany*, 50 (336), 1263–1266.

Dexter, A.R. and Hewitt, J.S., 1978. The deflection of plant roots. *Journal of Agricultural Engineering Research*, 23 (1), 17–22.

Dojarenko, A.G., 1924. The study of soil structure from the ratio of non-capillary and capillary porosity, and its significance in soil fertility. *Russ. J. Agric. Sci.*, 1, 451–474.

Donald, R., Kay, B., and Miller, M., 1987. The effect of soil aggregate size on early shoot and root growth of maize (Zea mays L.). *Plant and soil*, 103 (2), 251–259.

Drakopoulos, M., Connolley, T., Reinhard, C., Atwood, R., Magdysyuk, O., Vo, N., Hart, M., Connor, L., Humphreys, B., Howell, G., Davies, S., Hill, T., Wilkin, G., Pedersen, U., Foster, A., Maio, N. De, Basham, M., Yuan, F., and Wanelik, K., 2017. beamlines I12 : the Joint Engineering , Environment and Processing (JEEP) beamline at Diamond Light Source beamlines, (2015), 828–838.

FEI, 2015. User's guide Avizo ® 9 [online].

Fromm, H., 2019. Root Plasticity in the Pursuit of Water. *Plants*, 8 (7), 236.

Gao, W., Hodgkinson, L., Jin, K., Watts, C.W., Ashton, R.W., Shen, J., Ren, T., Dodd, I.C., Binley, A., Phillips, A.L., Hedden, P., Hawkesford, M.J., and Whalley, W.R., 2016. Deep roots and soil structure. *Plant Cell and Environment*.

Hadas, A., 1975. Water transfer to germinating seeds as afected by soil hydraulic properties and seed water contact impediments in Heat and Mass Transfer in the BiosphereIn. *Script Book, Wash—ington DC*, 501.

Hagin, J., 1952. Influence of soil aggregation on plant growth. *Soil Science*, 74 (6), 471–478.

Håkansson, I. and von Polgár, J., 1984. Experiments on the effects of seedbed characteristics on seedling emergence in a dry weather situation. *Soil and Tillage Research*, 4 (2), 115–135.

Hewitt, J.. and Dexter, A.., 1984. The behaviour of roots encountering cracks in soil: I1. Development of a predictive model. *Plant and Soil*, 28, 11–28.

Jabro, J.D., Iversen, W.M., Stevens, W.B., Evans, R.G., Mikha, M.M., and Allen, B.L., 2015. Effect of three tillage depths on sugarbeet response and soil penetrability resistance. *Agronomy Journal*, 107 (4), 1481–1488.

Jaggi, I.K., Gorantiwar, S.M., and Khanna, S.S., 1972. Effect of bulk density and aggregate size on wheat growth. *Journal of the Indian Society of Soil Science*, 20 (4), 421–423.

Karch, J., Dudák, J., Žemlička, J., Vavřík, D., Kumpová, I., Kvaček, J., Heřmanová, Z., Šoltés, J., Viererbl, L., Morgano, M., Kaestner, A., and Trtík, P., 2017. X-ray micro-CT and neutron CT as complementary imaging tools for non-destructive 3D imaging of rare silicified fossil plants. *Journal of Instrumentation*, 12 (12).

Kvasnikov, V. V, 1928. The structure of the soil and yields. *Russ. J. Agric. Sci*, 5, 459–482.

Logsdon, S.D., 2013. Root Effects on Soil Properties and Processes: Synthesis and Future Research Needs, 4, 173–196.

Logsdon, S.D., Parker, J.C., and Reneau, R.B., 1987. Root growth as influenced by aggregate size. *Plant and Soil*, 99 (2–3), 267–275.

Lynch, J.P., 2007. Roots of the second green revolution. *Australian Journal of Botany*, 55 (5), 493–512.

Mairhofer, S., Pridmore, T., Johnson, J., Wells, D.M., Bennett, M.J., Mooney, S.J., and Sturrock, C.J., 2017. X-Ray Computed Tomography of Crop Plant Root Systems Grown in Soil. *Current Protocols in Plant Biology*, 2 (December), 270–286.

Mawodza, T., 2019. Plant-soil interactions: the impact of plant water use efficiency on root architecture and soil structure. The University of Sheffield.

Mawodza, T., Burca, G., Casson, S., and Menon, M., 2020. Wheat root system architecture and soil moisture distribution in an aggregated soil using neutron computed tomography. *Geoderma*, 359, 113988.

Menon, M., Mawodza, T., Rabbani, A., Blaud, A., Lair, G.J., Babaei, M., Kercheva, M., Rousseva, S., and Banwart, S., 2020. Pore system characteristics of soil aggregates and their relevance to aggregate stability. *Geoderma*, 366, 114259.

Misra, R.K., Alston, A.M., and Dexter, A.., 1988. Root Growth and Phosphorus Uptake in Relation to the Size and Strength of Soil Aggregates. I. Experimental Studies, 11, 103–116.

Misra, R.K., Dexter, A.R., and Alston, A.M., 1986a. Penetration of soil aggregates of finite size. *Plant and Soil*, 94 (1), 59–85.

Misra, R.K., Dexter, A.R., and Alston, A.M., 1986b. Penetration of soil aggregates of finite size. *Plant and Soil*, 94 (1), 59–85.

Moradi, A.B., Hopmans, J.W., Oswald, S.E., Menon, M., Carminati, A., Lehmann, E., Anderson, S.H., and Hopmans, J.W., 2013. Applications of Neutron Imaging in Soil–Water–Root Systems, 113–136.

Nakamoto, T., 2002. Aggregate Size and Stability of Andosol as Affected by Soybean Root Growth under Controlled Conditions. *Plant Production Science*, 5 (4), 320–322.

Nimmo, J.R., 2004. Porosity and Pore Size Distribution. *Encyclopedia of Soils in the Environment*.

Octopus, 2019. Octopus reconstrsuction [online]. Available from: https://octopusimaging.eu/octopus/octopus-reconstruction [Accessed 1 Mar 2019].

Orosa-Puente, B., Leftley, N., von Wangenheim, D., Banda, J., Srivastava, A.K., Hill, K., Truskina, J., Bhosale, R., Morris, E., Srivastava, M., Kümpers, B., Goh, T., Fukaki, H., Vermeer, J.E.M., Vernoux, T., Dinneny, J.R., French, A.P., Bishopp, A., Sadanandom, A., and Bennett, M.J., 2018. Root branching toward water involves posttranslational modification of transcription factor ARF7. *Science*, 362 (6421), 1407–1410.

Poole, N., 2016. Germination and Emergence | Factors Affecting Germination. *Cereal growth stages guide*, (February).

Popova, L., Van Dusschoten, D., Nagel, K.A., Fiorani, F., and Mazzolai, B., 2016. Plant root tortuosity: An indicator of root path formation in soil with different composition and density. *Annals of Botany*, 118 (4), 685–698.

Puri, Y.P. and Qualset, C.O., 1978. Effect of seed size and seeding rate on yield and other characteristics of durum wheat. *Phyton*.

Ramachandran, G.N. and Lakshminarayanan, A. V., 1971. Three-dimensional reconstruction from radiographs and electron micrographs: application of convolutions instead of Fourier transforms. *Proceedings of the National Academy of Sciences of the United States of America*, 68 (9), 2236–2240.

Ries, S.K. and Everson, E.H., 1973. Protein content and seed size relationships with seedling vigor of wheat cultivars 1. *Agronomy Journal*, 65 (6), 884–886.

Robinson, B.H., Moradi, A., and Lehmann, E., 2008. Neutron Radiography for the Analysis of Plant – Soil Interactions. *Encyclopedia of Analytical Chemistry: Applications, Theory and Instrumentation*, 1–8.

Schneider, C. a, Rasband, W.S., and Eliceiri, K.W., 2012. NIH Image to ImageJ: 25 years of image analysis. *Nature Methods*, 9 (7), 671–675.

Schwarz, M., Cohen, D., and Or, D., 2010. Root-soil mechanical interactions during pullout and failure of root bundles. *Journal of Geophysical Research: Earth Surface*, 115 (4), 1–19.

Snyder, V.A. and Vázquez, M.A., 2005. Structure. *Encyclopedia of Soils in the Environment*, 4 (1958), 54–68.

Stirzaker, R.J., Passioura, J.B., and Wilms, Y., 1996. Soil structure and plant growth: Impact of bulk density and biopores. *Plant and Soil*, 185 (1), 151–162.

Suralta, R.R., Kano-Nakata, M., Niones, J.M., Inukai, Y., Kameoka, E., Tran, T.T., Menge, D., Mitsuya, S., and Yamauchi, A., 2018. Root plasticity for maintenance of productivity under abiotic stressed soil environments in rice: Progress and prospects. *Field Crops Research*, 220, 57–66.

Topp, C.N., 2016. Hope in change: The role of root plasticity in crop yield stability. *Plant Physiology*.

Tracy, S.R., Black, C.R., Roberts, J.A., McNeill, A., Davidson, R., Tester, M., Samec, M., Korošak, D., Sturrock, C., and Mooney, S.J., 2012. Quantifying the effect of soil compaction on three varieties of wheat (Triticum aestivum L.) using X-ray Micro Computed Tomography (CT). *Plant and Soil*, 353 (1–2), 195–208.

Tracy, S.R., Roberts, J.A., Black, C.R., McNeill, A., Davidson, R., and Mooney, S.J., 2010. The X-factor: Visualizing undisturbed root architecture in soils using X-ray computed tomography. *Journal of Experimental Botany*, 61 (2), 311–313.

Wadeson, N. and Basham, M., 2016. Savu: A Python-based, MPI Framework for Simultaneous Processing of Multiple, N-dimensional, Large Tomography Datasets.

Wang, M.-B. and Zhang, Q., 2009. Issues in using the WinRHIZO system to determine physical characteristics of plant fine roots. *Acta Ecologica Sinica*, 29 (2), 136–138.

Wang, X., Shen, J., Hedden, P., Phillips, A.L., Thomas, S.G., Ge, Y., Ashton, R.W., and Whalley, W.R., 2020. Wheat growth responses to soil mechanical impedance are dependent on phosphorus supply. *Soil and Tillage Research*, 205 (July 2020), 104754.

White, R.G. and Kirkegaard, J.A., 2010. The distribution and abundance of wheat roots in a dense, structured subsoil - Implications for water uptake. *Plant, Cell and Environment*, 33 (2), 133–148.

Whiteley, G.M. and Dexter, A.R., 1984. Displacement of soil aggregates by elongating roots and emerging shoots of crop plants. *Plant and Soil*, 77 (2–3), 131–140.

Whiteley, G.M., Hewitt, J.S., and Dexter, A.R., 1982. The buckling of plant roots. *Physiologia Plantarum*, 54 (3), 333–342.

Xu, W., Cui, K., Xu, A., Nie, L., Huang, J., and Peng, S., 2015. Drought stress condition increases root to shoot ratio via alteration of carbohydrate partitioning and enzymatic activity in rice seedlings. *Acta Physiologiae Plantarum*, 37 (2).

Zarebanadkouki, M., Kim, Y.X., and Carminati, A., 2013. Where do roots take up water? Neutron radiography of water flow into the roots of transpiring plants growing in soil. *New Phytologist*, 199 (4), 1034–1044.

Table 1 Physicochemical properties of the aggregate fractions used in plant growth experiments

								Exchangeable base cations (NH4OAc) (mg/100g)					cmol (+)/kg
	pH	EC (µS/cm)	%SOM	%Sand	%Silt	%Clay	%N	Na	K	Ca	Mg	P (mg/kg soil)	CEC
Bulk soil	6.8	205	5.59	70	16	14	0.19	3.02	27.85	349.50	28.35	35.49	20.63
<0.25 mm	6.9	262	5.51	___	___	___	0.22	___	___	___	___	28.00	___
0.25-0.5 mm	7.0	182	3.58	74	14	12	0.14	2.04	26.20	283.00	22.50	25.64	16.74
0.5-1mm	7.0	119	6.58	___	___	___	0.19	___	___	___	___	25.59	___
1-2 mm	7.1	227	5.96	___	___	___	0.21	___	___	___	___	44.91	___
2-4 mm	6.6	200	6.49	68	18	14	0.20	2.61	30.70	417.00	32.80	43.14	24.41
Avg of agg fractions	6.9	198	5.62				0.19					33.46	

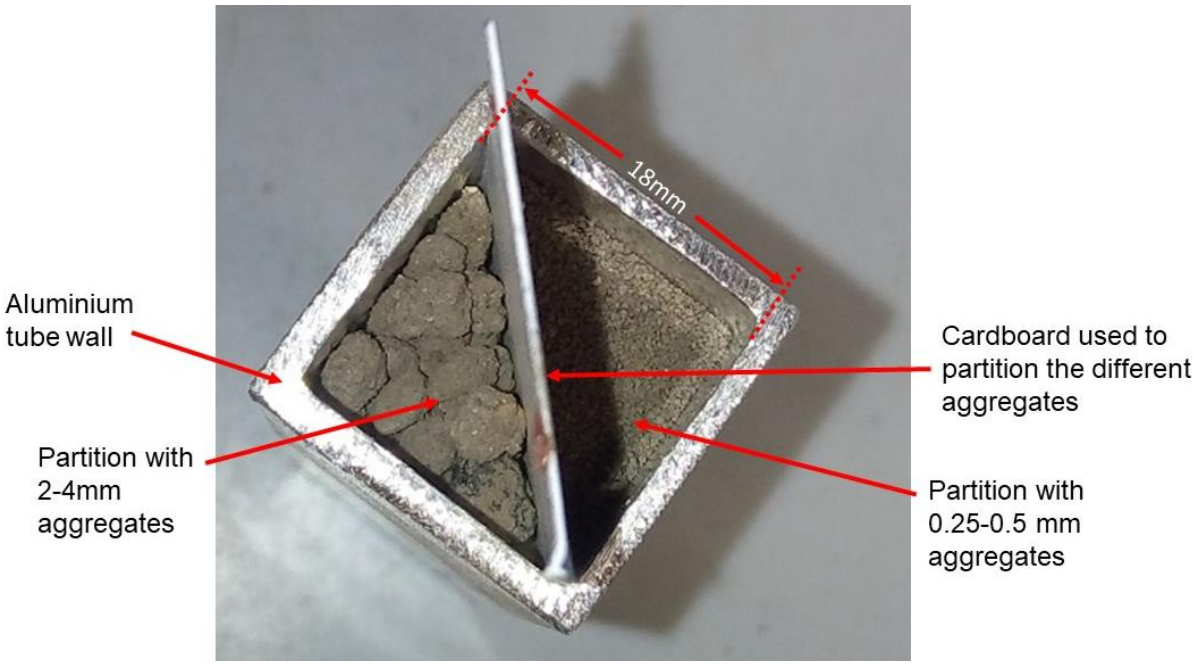

Figure 1 Aluminium container showing the set-up of the partitioned aggregates before the removal of the separating cardboard

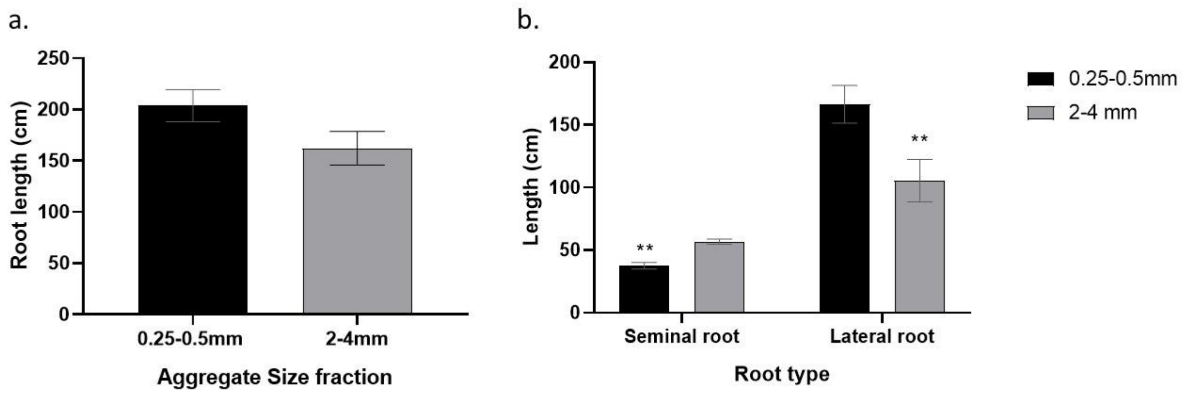

*Figure 2 a) Plant biomass and b) root: shoot ratio of 14-day old wheat plants grown in the different aggregate size classes. (n=3). The error bars indicate Standard Error of the mean. Symbols indicate a significant difference between means in t-tests (** p =≤0.01)*

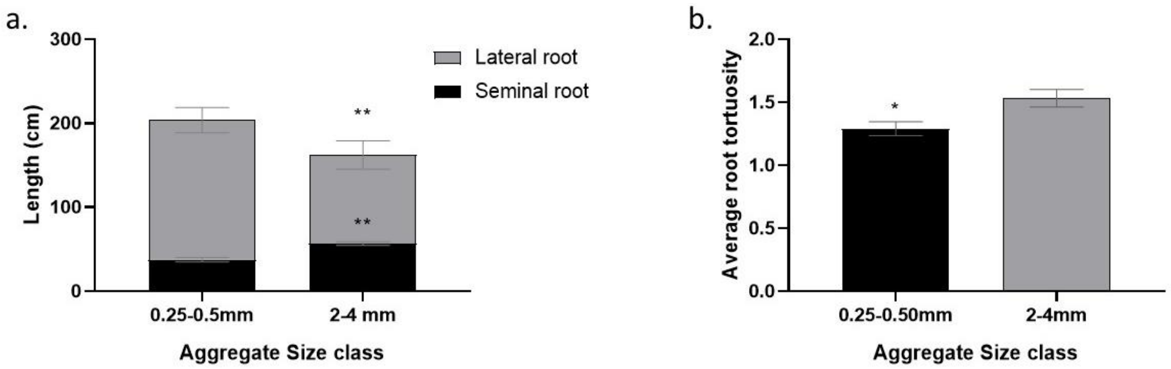

Figure 3 a) Total root length and b) average root tortuosity of 14-day old wheat seedlings growing in 0.25-0.5 and 2-4 mm aggregates (n=3). The error bars indicate Standard Error of the mean for seminal and lateral roots. Symbols indicate a significant difference between means in t-tests (=≤0.05, **=≤0.01)*

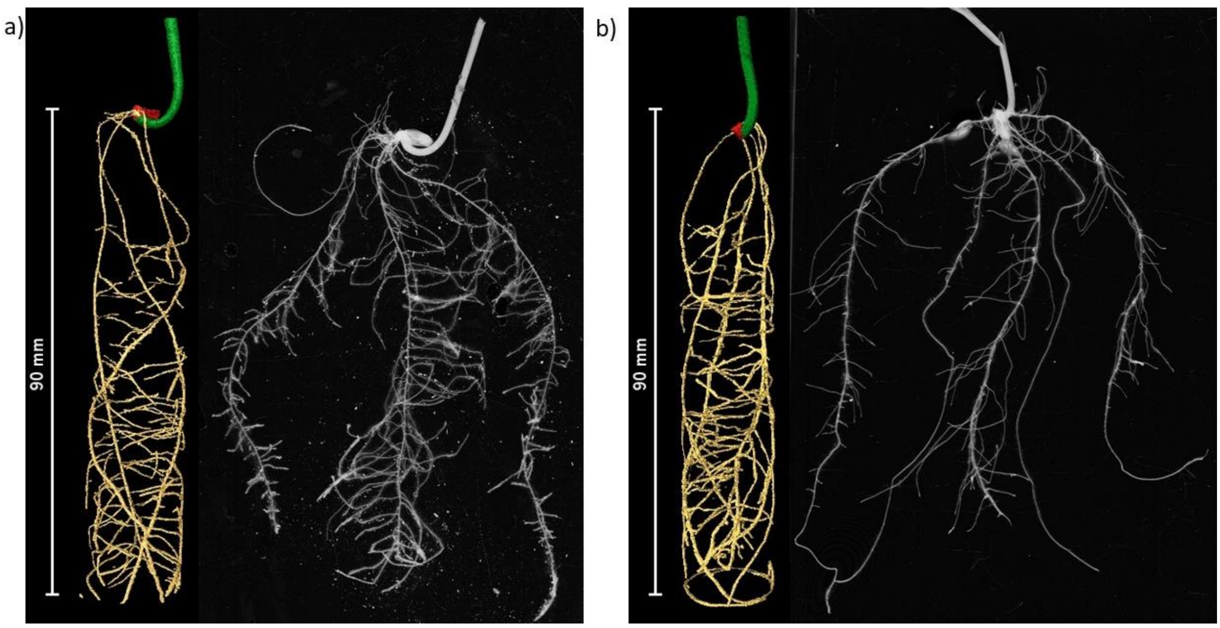

Figure 4 Neutron CT and corresponding flatbed scan images of two selected replicates of the 14 day old wheat seedlings growing in a) 0.25-0.5 mm and b) 2-4 mm aggregates. The scale bar applies only to the NCT image on the left of each replicate.

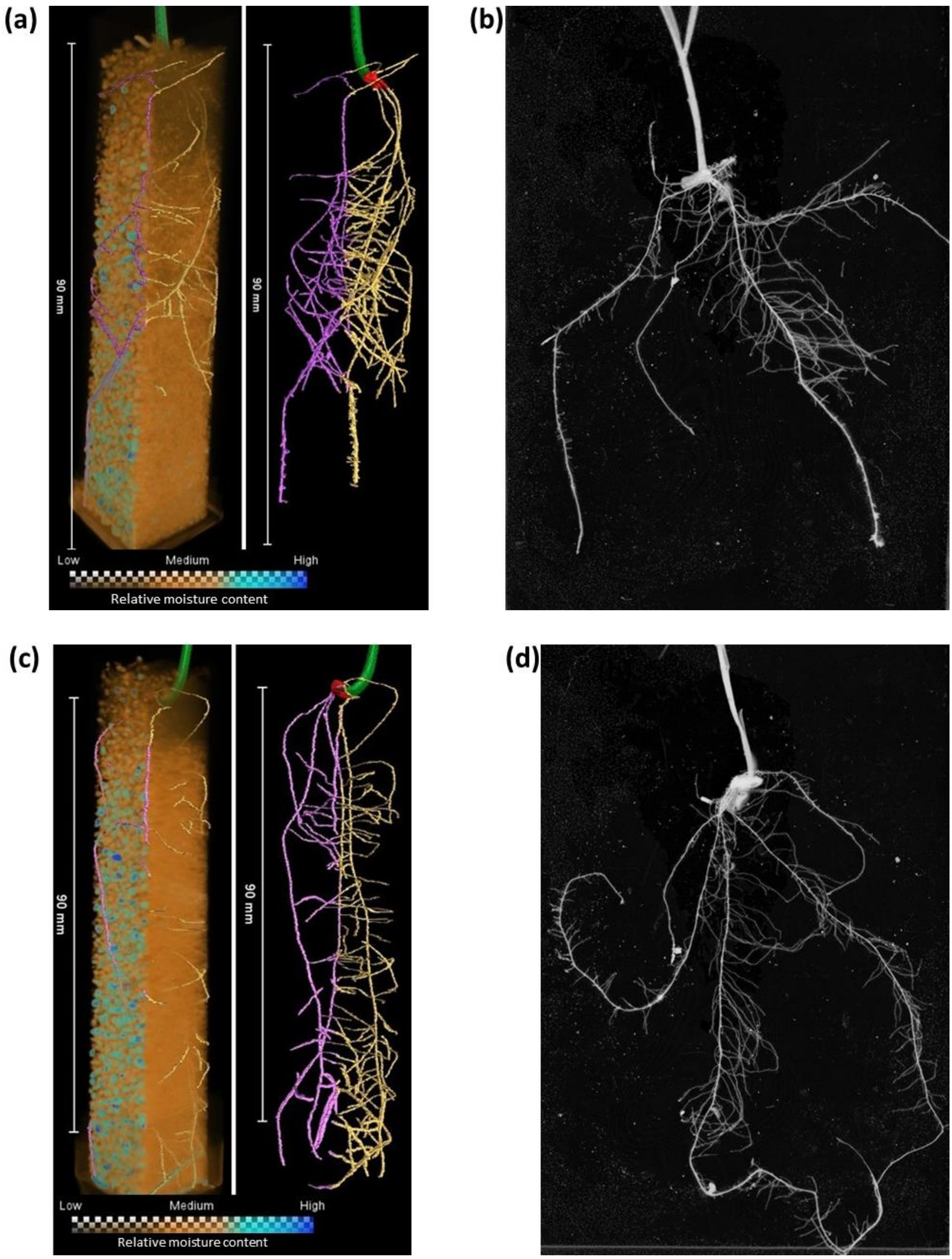

Figure 5 a, c) Showing neutron CT images of two 14 day old wheat seedlings growing in partitioned prisms with aggregates of 0.25-0.5 (right) and 2-4 (left) mm on either side of each tube. Relative soil moisture distribution in each side is given to the left of each level whilst the extracted root is given on the right. Roots growing in each of the different aggregates are coloured differently with purple being used to indicate roots growing in 2-4 mm aggregates whilst yellow is used for indicate roots growing in 0.25-0.5 mm aggregates. b, d) show flatbed scan images of the corresponding plants after washing.

Table 2 Root properties from plants grown in partitioned aggregates

	Root Length (mm)		Root Volume (cm^3)		Surface area (cm^2)		Average root diameter(mm)	
Aggregate size	0.25-0.5	2-4	0.25-0.5	2-4	0.25-0.5	2-4	0.25-0.5	2-4
Plant 1	93.67	57.66	0.0998	0.0520	12.89	7.84	0.337	0.290
Plant 2	114.60	57.52	0.1036	0.0747	13.95	8.63	0.326	0.398

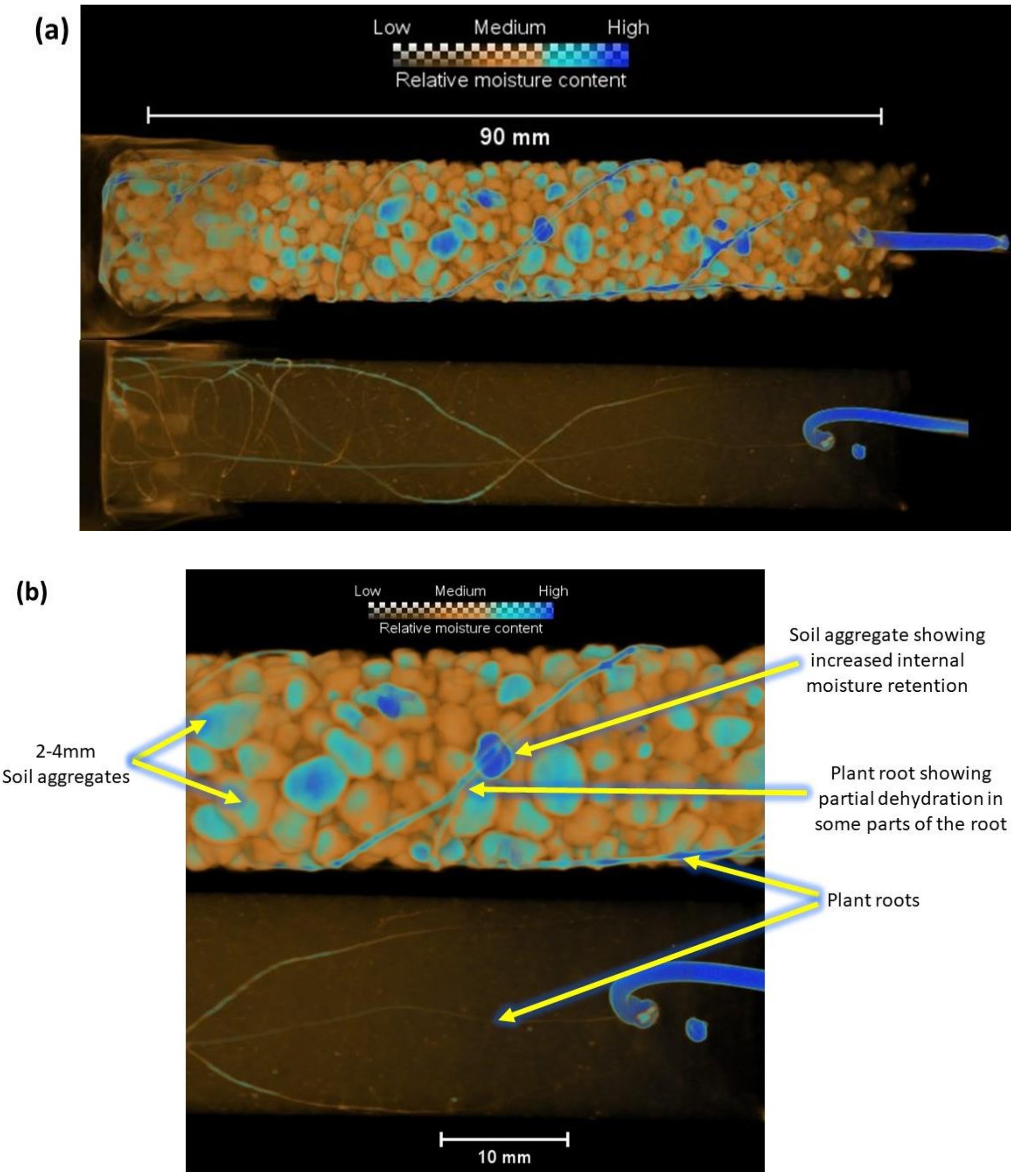

Figure 6 Showing relative moisture distribution in the two different aggregate sizes used for experimentation at the time of imaging with the blue colour showing increased moisture content. a) Shows the moisture distribution within the whole soil growth column whilst b) shows a more detailed close up view of the two tubes indicating resolvable roots and other finer soil features

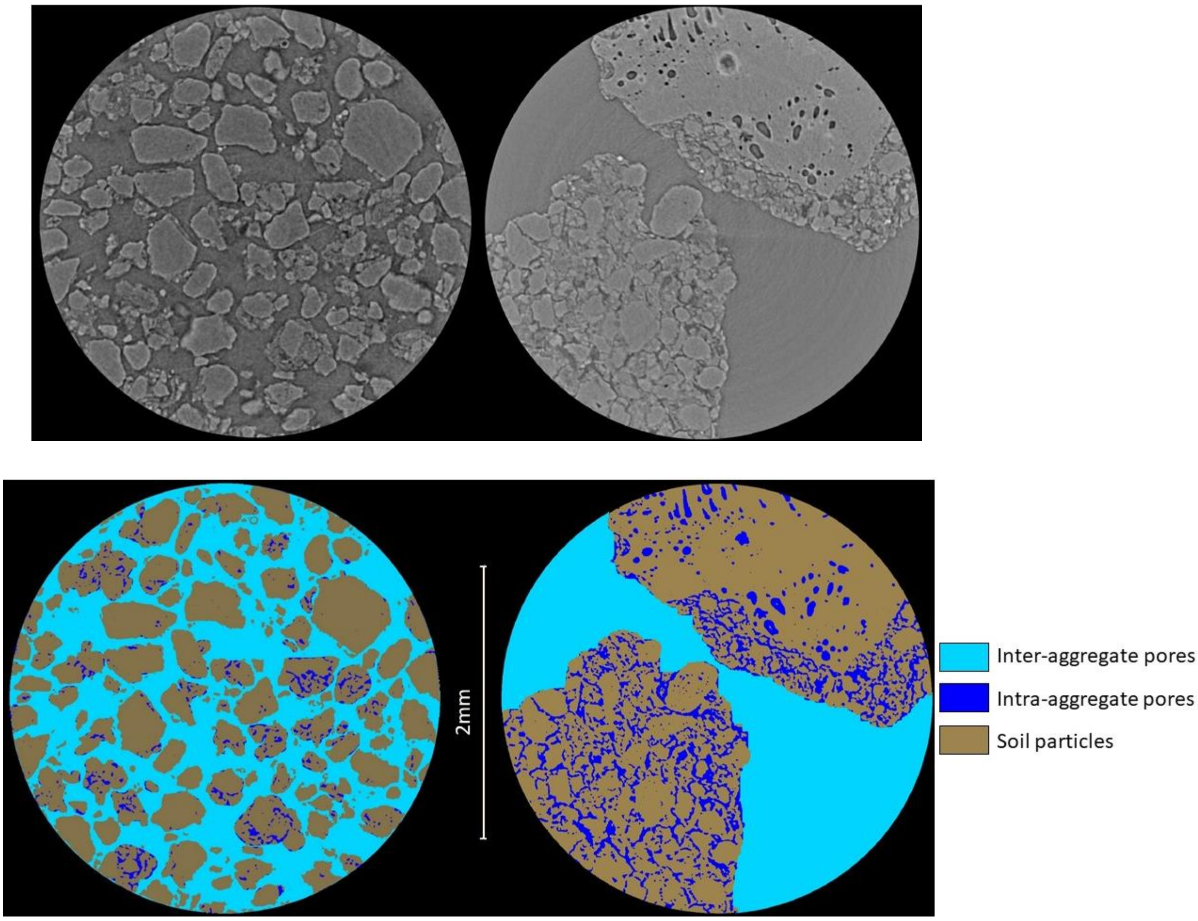

Figure 7: X-Ray synchrotron image of 0.25-0.5 (left) and 2-4mm (right) aggregates showing both inter- and intra- aggregate pore spaces

Table 3 Showing a breakdown of pore distribution in the different aggregate size classes as determined from the X-Ray synchrotron images

	% Inter-aggregate pores	% Intra-aggregate pores	Total porosity (m^3/m^3)
0.25-0.5 mm	94.39	5.61	0.547
2-4 mm	77.67	22.33	0.653

Supplementary data

A. Preliminary screening for differences in plant properties

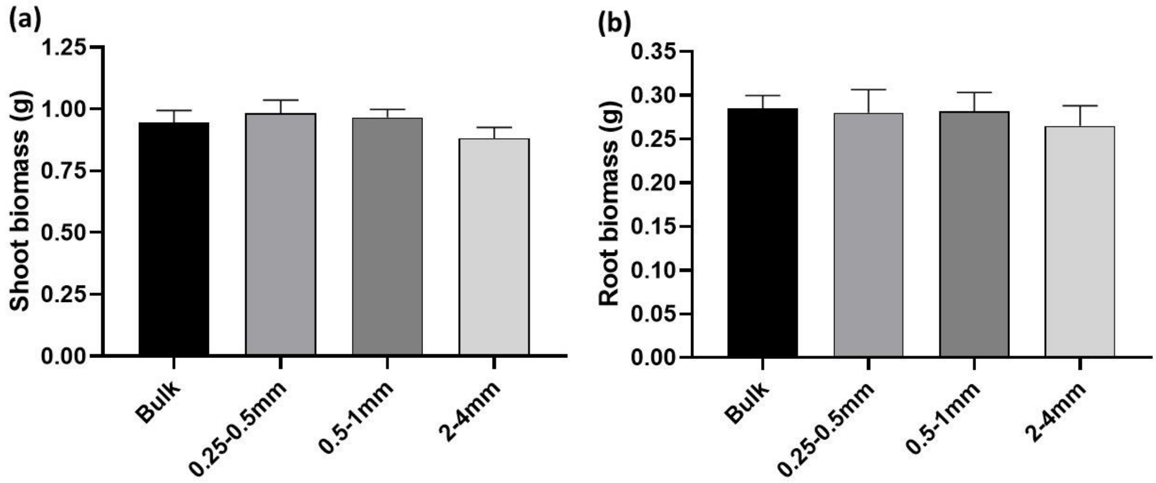

Figure 1: Shoot (a) and root (b) biomass of 4week old wheat plants grown in aggregates of different sizes

In this preliminary experiment, each of the four macro-aggregate size fractions (0.25-0.5, 0.5-1, 2-4mm), along with the bulk (<4mm sieved soil) were filled into 435cm^3 cylindrical pots (68mm diameter × 120mm height). A single wheat (*Triticum Aestivum*. L cv. Fielder) seed was planted about 1cm underneath the surface of the soil and the pots were watered to a volumetric moisture content (θ) of between 16 and 20%. This water content was maintained during the course of this experiment by surface irrigation to the predetermined weight corresponding to the above mentioned θ. These plants were grown for four weeks in a growth chamber maintained at a temperature of 22°C (day)/18°C (night) and a relative humidity of 55% with light intensity averaging 400µmol m^2 s^{-1}. After this growth period, the plants were harvested and their shoots were excised and dried in an oven at 60°C for 48 hours to obtain dry root and shoot biomass. In this initial screening of the wheat seedlings did not show significant differences in root and shoot properties. This was probably due to the greater amount of time used to grow the plants which could have had an effect of masking the subtle differences in plant growth. This may have happened due to the limited volume for root growth thus any differences that were seen early on became subtle as the plants grew. However the most contrasting differences in root growth were seen between the largest 2-4mm and smallest 0.25-0.5mm aggregate sizes and thus these were used for further experimentation.

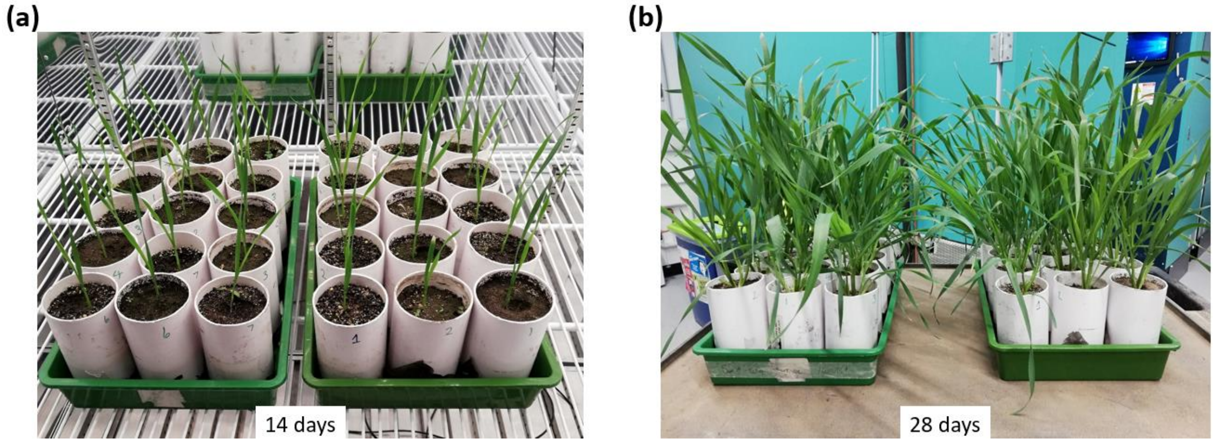

Figure 2 Preliminary experiment showing wheat plants growing in different size aggregates at a) 14 days and b) 28 days

B. Plant neutron CT scans

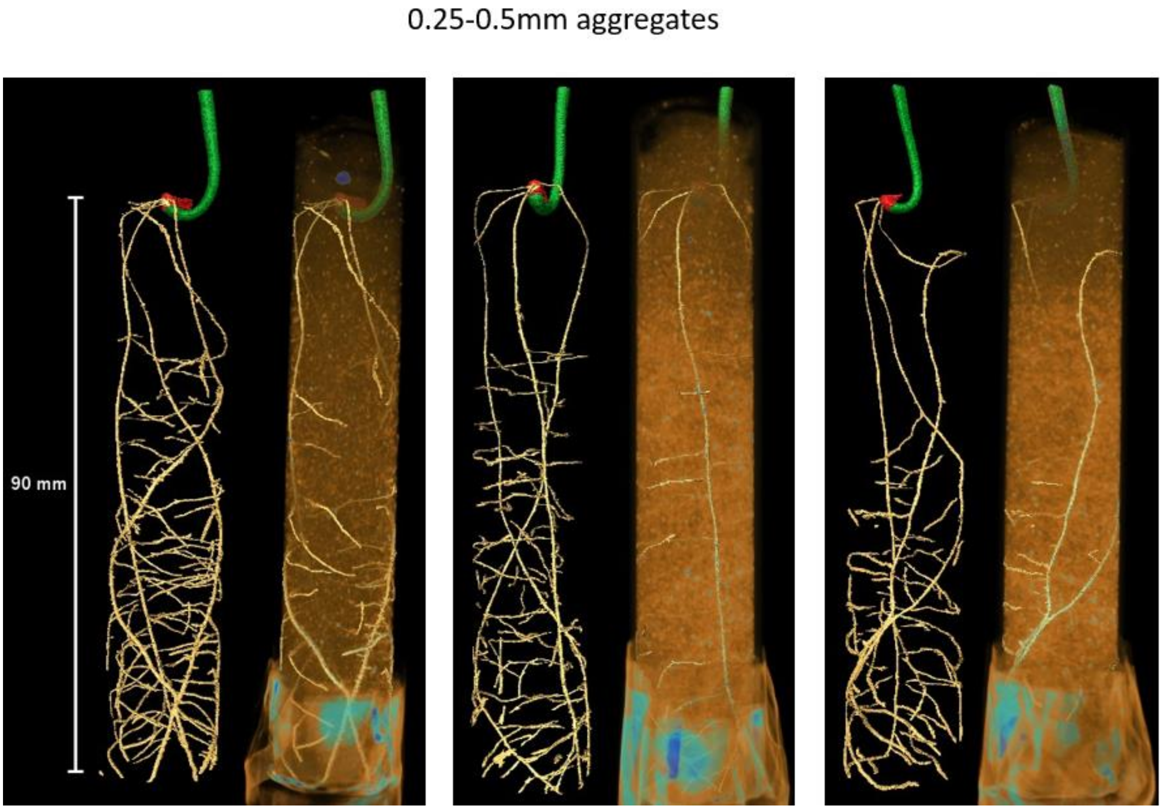

2-4 mm aggregates

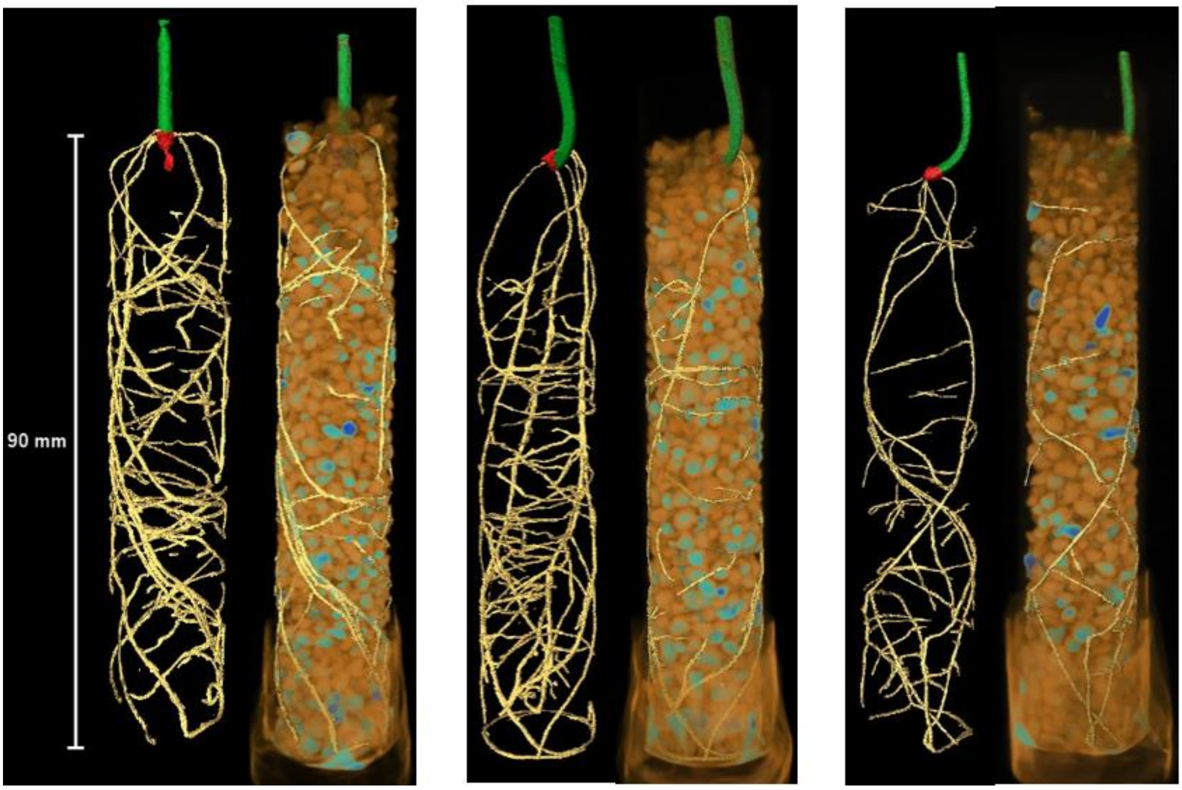

Table S1 Selected root properties from experiment with individual aggregates grown separately

	0.25-0.5 mm	**2-4 mm**
Root thickness (mm)	0.59 ± 0.02*	0.47 ± 0.01
Root: Shoot ratio (-)	0.83 ± 0.02*	0.69 ± 0.04
Specific root length (mm g^{-1})	88.44 ± 2.54	94.81 ± 3.81*
Root tissue density (cm^3 g^{-1})	25.02 ± 1.30*	16.78 ± 1.20
Root branching density (roots cm^{-1})	1.02 ± 0.04	1.27 ± 0.06